INFRARED SPECTRA OF LUNAR SOIL ANALOGS

(Contract No. NASW-2918)

By

J. R. Aronson, E. M. Smith, and P. F. Strong

July 1977

ARTHUR D. LITTLE, INC.

Arthur D Little, Inc.

ABSTRACT

This report describes the results of an investigation of the infrared spectra of analogs of lunar soils. The purpose of the investigation was to further the development of methodology for interpretation of remotely measured infrared spectra of the lunar surface. To this end we have (1) obtained the optical constants of dunite, bytownite, augite, ilmenite, and a mare glass analog, (2) measured the infrared emittance spectra of powdered minerals, and (3) compared these with spectra calculated by our reflectance theory using our catalogue of optical constants. The results indicate that the predictions of the the ry closely simulate the experimental measurements if the optical constants are properly derived.

TABLE OF CONTENTS

LIST OF FIGURES

I. INTRODUCTION

Remote measurements of the infrared emittance spectra of planetary surfaces have the potential for mapping the mineral composition of those surfaces. This has been evident for many years as the molecular and lattice vibrations which make up the infrared spectrum provide characteristic signatures of mineral composition.[1] However, emittance or reflectance signatures are characteristic not only of the mineralogy but of various physical parameters of the surface such as particle size, shape, and packing density. These physical parameters are so important that the same material may have either a spectral peak or trough at the same frequency depending on particle subdivision for example.[2] This apparent indeterminancy together with the great number of possible mineral species poses a serious difficulty in the utilization of remote infrared spectroscopy as an analytical tool.

To remedy this problem we developed a theory of the spectral reflectance and emittance of particulate surfaces[3,4,5] that is capable of predicting their signatures. The theory was developed and tested using relatively few model minerals since optical constants were not available for a wide number of mineral species. In order to use the theory together with infrared measurements to interpret the spectrum of the lunar surface, the optical constants of relevant mineral types need to be obtained. The more detailed the catalogue of optical constants is made, the more subtle the interpretation of the composition of planetary surface is possible.

The infrared spectra of minerals can be considered to be a combination of the effects of structural type (olivines, pyroxenes, feldspars, etc.) and variations caused by cation composition within homologous series. Estep et al[6,7] have shown the kind of subtle distinctions possible when lunar samples are available in the laboratory, as the effects of the physical parameters referred to above can be circumvented by sample preparation. Whether some of the subtle effects can be measured in remote data, however, remains to be demonstrated.

1

Arthur D Little, Inc.

The wealth of information inherently present in the middle and far infrared spectral regions when compared to the complementary near infrared and visible regions already successfully exploited by Adams, McCord, Pieters, and coworkers[8] suggests that a significant effort in this region will lead to valuable results.

Our work during this contract has been focussed on two principal tasks. The first was to obtain optical constants for suitable lunar analogs so as to prepare for eventual interpretation of remotely obtained lunar spectra. The second task was to use these optical constants together with our theory to simulate the signatures expected from particulate samples and to compare these predictions with laboratory measurements on powders of the analog materials. The purpose of this task was to ascertain the degree to which lunar spectra could presently be interpreted and to suggest areas where further theoretical improvements need to be made.

Arthur D Little, Inc.

II. ANALOG SAMPLES

The choice of analogs to study in this program was greatly facilitated by many discussions with our co-investigator, Dr. David S. McKay of the Johnson Space Center, and his colleagues. In addition Dr. McKay obtained analytical information as to the chemistry of our samples, provided many of them including the powders that we studied, and had some measurements of particle size distributions made for us.

There were several problems associated with choice of samples for this program. We obtain the optical constants (the real and imaginary components of the complex index of refraction) by fitting the reflectance spectrum of a polished sample using classical dispersion theory (Lorentz lines) as previously described.[9] For this purpose we need a polished sample of several cm^2 area and homogeneous composition. Ideally a single crystal of known orientation should be measured. For biaxial crystals, three sets of optical constants exist, so that three separate measurements need to be made using polarized radiation. Monoclinic and triclinic crystals do not have a set of optic axes that are independent of wavelength so that the problem is very complicated. On a practical level, obtaining large enough single crystals so that the three measurements could be made for samples of lunar composition is also formidable. At the same time we need to have sufficient sample so that powders can be produced of specified particle size distributions for each sample of interest.

Several of these problems might be ameliorated by using randomly oriented polycrystalline samples and treating them as homogeneous isotropic samples. However, such a procedure is not rigorous for several reasons. First, such a sample will invariably produce some scattering owing to microcracks and interfaces between crystals. Second, the assumption of random distribution is always in question. Another drawback is that using the Fresnel equations to fit the spectrum assumes a facet model of the surface, and the quantity being averaged by the

3

measurement is the reflectance. Subsequent derivation of the optical
constants from the averaged reflectances of the facets produces a set
of optical constants that are required to be appropriate in the calcu-
lations of our particulate theory (where cross-sections are the quan-
tities to be averaged). This requirement would not appear to be met
for mixtures of different minerals where, for instance, the true
refractive indices of different substances may at some frequency be
disposed above and below unity. The derived optical constants would
appropriately represent the coherent surface (Fresnel) reflectance of
the particles in the mixture but not necessarily the refractive part of
the scattering. It is easy to see that averaging of the individual
optical constants themselves would fail as it would be possible to con-
struct a case based on averaged optical constants where little reflec-
tance or scattering would be predicted to occur ($\bar{n} \sim 1$) even though
both components were good reflectors. At any rate the refractive
scattering contributions to the particle cross sections in our theory
would not seem to be appropriate owing to the averaging process inherent
in deriving the optical constants. The extent to which this problem is
important will be examined in this work by a comparison of spectra
predicted by our theory for quartz particles using both the optical
constants of quartz[10] and those derived herein for quartzite.

The samples studied on this program were:

1. <u>Mare glass analog</u>

This sample was prepared by Dr. J. F. Wosinski of Corning
Glass Works, Corning, New York. It was prepared under reducing
conditions (charcoal) in order to simulate lunar conditions. The
chemical composition determined by X-ray fluorescence by M. Rhodes
and K. Rodgers is as follows:

SiO_2	44.65	MgO	7.38
TiO_2	6.59	CaO	12.25
Al_2O_3	13.42	Na_2O	<0.05
Cr_2O_3	0.14	K_2O	0.02
FeO	13.95	P_2O_5	0.02
MnO	0.14	S	0.02
		Total	98.58

4

Ferrous iron was also determined by wet chemistry to be 13.29. This indicates that, within analytical error, all of the Fe is present as FeO. The glass proved to be slightly inhomogeneous when analyzed with the probe, but not enough to matter. The chemical composition is fairly close to that of Apollo 11 soil 10084.

2. Dunite

The dunite sample is Ward's #44 from Jackson County, North Carolina. It was analyzed with the energy dispersive X-ray spectrometer using other olivine minerals as standards. It is Fo_{91}. This dunite contains minor spinel inclusions.

3. Pyroxenite

The pyroxenite sample was obtained from the Harvard University collection through the courtesy of Prof. Clifford Frondel. It was a fine grained sample and was analyzed by electron probe. Its partial composition is as follows (three points):

CaO	FeO	MgO
22.14	9.70	12.33
20.86	11.41	12.06
21.52	9.85	12.42

The mol percent of pyroxene end members corresponding to these three points is Wo_{47}, En_{37}, Fs_{16}; Wo_{45}, En_{36}, Fs_{19}; Wo_{46}, En_{37}, Fs_{17}. This is roughly a diopside composition (actually a salite).

In addition the sample contains minor (<5%) pigeonite. One analyzed point gave Wo_2, En_{57}, Fs_{41}. This is a hypersthene composition.

4. Bytownite

The bytownite sample is Ward's #277 from Crystal Bay, Minnesota. Its composition is $An_{76}Ab_{24}Or_0$. It has less than 0.1% FeO and K_2O.

5. Ilmenite

A large grained polycrystalline ilmenite sample was obtained from Ward's Natural Science Establishment Inc. It came from Baie St. Paul, Quebec. It contains some lamellae which are titanomagnetite.

Arthur D Little Inc

6. Augite

Prof. Frondel supplied us with a polycrystalline augite sample (#116154) from Oaxaca, Oaxaca, Mexico. Its composition was found to be $Wo_{52.4}$ $En_{40.6}$ $Fs_{7.0}$, which is actually a diopside. The probe analysis results are:

SiO_2	50.04	MnO	0.24
TiO_2	0.29	MgO	13.43
Al_2O_3	7.49	CaO	24.03
Cr_2O_3	0.0	Na_2O	0.36
FeO	4.10		

7. Quartzite

We obtained a pink quartzite sample from Dell Rapids, South Dakota, from Ward's National Science Establishment. Prof. Frondel examined it and felt it was as pure as we were likely to find. He indicated that the pink color represents about 0.05% iron. EDX analysis showed no observable peaks so the sample is pure to less than 0.5%

8. Dunite

A sample from Ward's labeled pyroxenite #43 (Harzburgite) from Nye, Montana, turned out to consist primarily of olivine. The composition of the olivine is Fo_{87}. Oxide weight percents are as follows:

MgO	46.56
SiO_2	39.84
CaO	0.07
FeO	12.14
Total	98.61

6

III. OPTICAL CONSTANTS

As mentioned previously we obtained the optical constants of our samples as described in reference 9 with the exception that all of the samples measured in this work were measured relative to a gold mirror on our Perkin-Elmer 521 Spectrophotometer at a 30° angle of incidence. A Perkin-Elmer wire grid polarizer[11] was used to measure the instrumental polarization. The pyroxenite optical constants were measured previously.[9]

The Lorentz line parameters and their estimated standard deviations. for our samples are:

TABLE I - MARE GLASS ANALOG $\varepsilon_\infty = 2.6759 \ (0.226)$

ν_i		γ_i		S_i	
429.01	(2.56)	0.6154	(.0190)	2.9960	(.0913)
913.01	(3.42)	0.08827	(.0182)	0.2222	(.0837)
974.69	(10.28)	0.1813	(.0092)	0.4454	(.0965)

TABLE II - DUNITE $\varepsilon_\infty = 2.4177 \ (.0945)$

1029.01	(1.60)	0.05468	(.00516)	0.04237	(.00473)
971.66	(.62)	0.01210	(.00284)	0.00788	(.00125)
881.26	(1.54)	0.02942	(.00111)	0.53153	(.03359)
836.34	(2.12)	0.01705	(.00726)	0.04567	(.02155)
691.36	(17.88)	0.10327	(.09424)	0.07026	(.05835)
612.08	(2.81)	0.04388	(.01136)	0.06609	(.01927)
544.76	(6.54)	0.07002	(.02168)	0.06837	(.04321)
521.89	(2.12)	0.02686	(.02169)	0.08655	(.06850)
503.09	(1.25)	0.04214	(.00777)	0.25336	(.05476)
467.09	(1.38)	0.04921	(.01302)	0.13440	(.04162)
443.19	(1.28)	0.03301	(.01001)	0.06214	(.02338)
412.61	(1.69)	0.04094	(.00922)	0.61551	(.21155)
396.65	(2.02)	0.05012	(.01491)	0.62872	(.24842)
359.08	(1.48)	0.06157	(.01003)	0.90098	(.12326)
297.04	(1.84)	0.05984	(.01109)	0.88819	(.17169)

TABLE III - BYTOWNITE ϵ_∞ = 2.1414 (.0536)

ν_i		γ_i		s_i	
1108.60	(1.70)	0.07523	(.00494)	0.07916	(.00760)
978.62	(5.00)	0.10196	(.01038)	0.21047	(.05198)
918.65	(1.96)	0.06153	(.00650)	0.40343	(.04245)
736.43	(6.41)	0.10044	(.03057)	0.09096	(.02369)
623.62	(2.10)	0.06225	(.01196)	0.10150	(.03167)
581.40	(1.13)	0.07619	(.00978)	0.44074	(.05858)
545.88	(1.11)	0.03266	(.00658)	0.11306	(.02551)
484.38	(2.67)	0.02920	(.01845)	0.01884	(.01615)
467.24	(3.13)	0.04955	(.01939)	0.04398	(.02179)
423.89	(1.07)	0.06315	(.00981)	0.16746	(.03862)
384.04	(1.37)	0.13021	(.01497)	0.82576	(.08395)
313.78	(5.88)	0.08327	(.05903)	0.09668	(.07012)

TABLE IV - ILMENITE ϵ_∞ = 6.0789 (.0492)

1032.76	(21.91)	0.10150	(.05765)	0.04842	(.02192)
673.46	(3.74)	0.13277	(.01638)	0.09840	(.01592)
618.91	(.67)	0.04325	(.00293)	0.13381	(.00938)
509.69	(.69)	0.10528	(.00350)	1.16467	(.05555)
434.23	(.71)	0.16240	(.00478)	3.50175	(.08687)
266.81	(1.21)	0.22768	(.00591)	16.09684	(.36622)

TABLE V - AUGITE ϵ_∞ = 2.4505 (.0703)

1058.87	(1.17)	0.03689	(.00186)	0.11180	(.01030)
999.09	(3.70)	0.04831	(.01632)	0.04173	(.01693)
944.07	(2.10)	0.04404	(.00923)	0.12652	(.04239)
900.05	(2.31)	0.06063	(.00872)	0.32607	(.04918)
678.67	(12.95)	0.05093	(.06868)	0.02679	(.02120)
630.71	(3.42)	0.02522	(.01496)	0.02085	(.01184)
540.58	(2.55)	0.07988	(.01003)	0.14215	(.03523)
504.26	(1.47)	0.06663	(.01127)	0.33870	(.08368)
471.41	(1.58)	0.07326	(.01182)	0.45630	(.08154)
426.11	(2.13)	0.04066	(.02175)	0.05935	(.04171)
399.20	(1.21)	0.08558	(.01188)	0.61875	(.07343)
336.95	(1.35)	0.07524	(.01041)	0.58360	(.07470)

TABLE VI – QUARTZITE $\quad \varepsilon_\infty = 2.4079 \ (.0599)$

ν_i		γ_i		S_i	
1160.88	(.62)	0.00842	(.00133)	0.00683	(.00074)
1066.14	(1.08)	0.01627	(.00072)	0.65264	(.01887)
797.60	(1.06)	0.01525	(.00355)	0.04914	(.01739)
780.95	(1.37)	0.01737	(.00543)	0.09702	(.02587)
690.62	(5.81)	0.03364	(.02482)	0.04008	(.02747)
536.24	(.98)	0.03676	(.00390)	0.07188	(.00660)
474.73	(1.09)	0.02591	(.00445)	0.21353	(.07325)
461.57	(.69)	0.02109	(.00393)	0.72588	(.07343)
399.15	(.50)	0.01808	(.00360)	0.15622	(.02287)
379.90	(.81)	0.02671	(.00531)	0.45192	(.05980)

The range of applicability for these oscillator parameters is between $300 \ \mathrm{cm}^{-1}$ and $1500 \ \mathrm{cm}^{-1}$.

Comparison of the data for our bytownite sample ($An_{76}Ab_{24}$) with that previously obtained for anorthosite ($An_{47}Ab_{50}Or_3$, according to electron probe analysis) indicates a general pattern similarity as might be expected from Lyon's[12] transmittance data. While there are some differences in minor features, there seems to be a clear correspondence between the following features for the two feldspars:

An_{76}				An_{47}		
ν	γ	S		ν	γ	S
1108.60	.07523	.07916		1077.4	.0862	.118
978.62	.10196	.21047		979.7	.1022	.208
918.65	.06153	.40343		919.8	.1019	.495
736.43	.10044	.09096		723.2	.1681	.214
581.40	.07619	.44074		585.8	.1466	.410
545.88	.03266	.11306		528.9	.0704	.197
384.04	.13021	.82576		392.6	.2232	1.291
313.78	.08327	.09668		330.4	.1044	.189

Data for a third composition would be required to establish a trend with cation composition such as that suggested by Angino[13] for the far infrared spectrum.

In the same way a comparison between the "augite" ($Wo_{52}En_{41}Fs_7$) data obtained during this work and the "diopsidic" pyroxenite

Arthur D. Little, Inc.

($Wo_{46}En_{37}Fs_{17}$) previously studied[9] indicates an even closer correspondence undoubtedly owing to the smaller discrepancy in cation ratios.

$Wo_{46}En_{37}Fs_{17}$				$Wo_{52}En_{41}Fs_7$		
ν	γ	S		ν	γ	S
1077.2	0.0324	0.151		1058.87	0.03689	0.11180
1006.8	0.0326	0.032		999.09	0.04831	0.04173
951.3	0.0386	0.113		944.07	0.04404	0.12652
904.5	0.0532	0.545		900.05	0.06063	0.32607
634.8	0.0469	0.066		630.71	0.02522	0.02085
542.1	0.0814	0.269		540.58	0.07988	0.14215
507.3	0.0441	0.345		504.26	0.06663	0.33870
480.0	0.0599	0.439		471.41	0.07326	0.45630
433.6	0.0236	0.039		426.11	0.04066	0.05935
401.5	0.0875	0.754		399.20	0.08558	0.61875
333.1	0.0579	0.584		336.95	0.07524	0.58360

Unlike the case of the feldspars above, the small cation differences in these pyroxenes are unlikely to be distinctive enough to be measured remotely.

The oscillator parameters are used to generate the optical constants by using the equation:

$$m^2 = \varepsilon_\infty + \sum_{j=1}^{n} \frac{S_j}{1 + i\,\gamma_j\left(\frac{\nu}{\nu_j}\right) - \left(\frac{\nu}{\nu_j}\right)^2}$$

where m is the frequency dependent complex index of refraction, $m = n - ik$, S_j is the line strength, ν_j its frequency, and γ_j the damping for each resonance j. ε_∞ is the high frequency dielectric constant.

Figures 1 - 6 show the fits obtained between the experimental measurements of the polished samples and the spectra calculated from the optical constants derived from the Lorentz line parameters given in the tables. Somewhat better fits might be obtained by digitizing many more points for each spectrum. The apparent extra resonance in quartzite near 450 cm^{-1} would have required considerably more effort to remedy than the data appears to warrant.
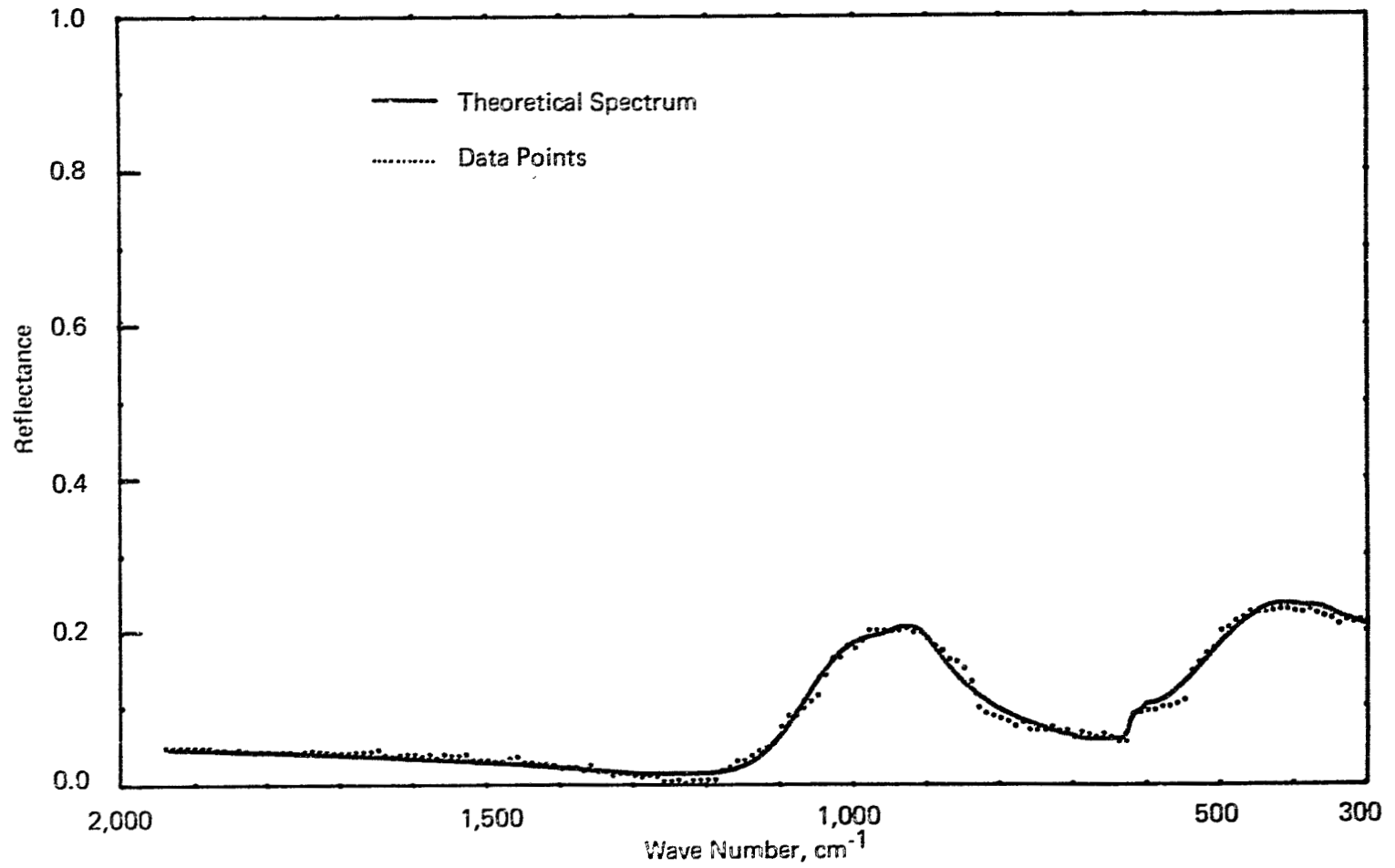
Arthur D. Little, Inc.

FIGURE 1   REFLECTANCE SPECTRUM OF MARE GLASS FITTED WITH
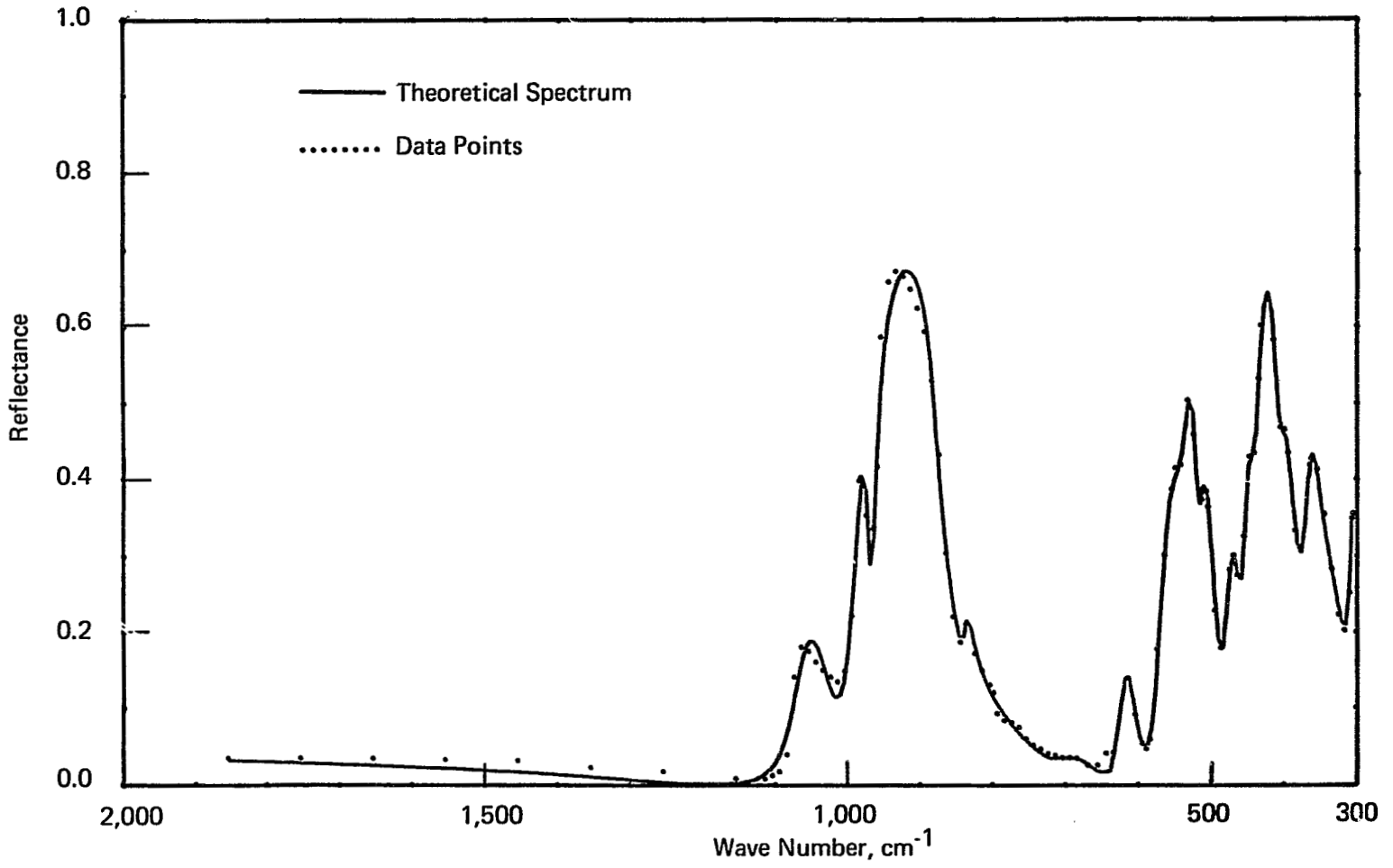THREE LORENTZ LINES

FIGURE 2   REFLECTANCE SPECTRUM OF DUNITE FITTED WITH FIFTEEN LORENTZ LINES
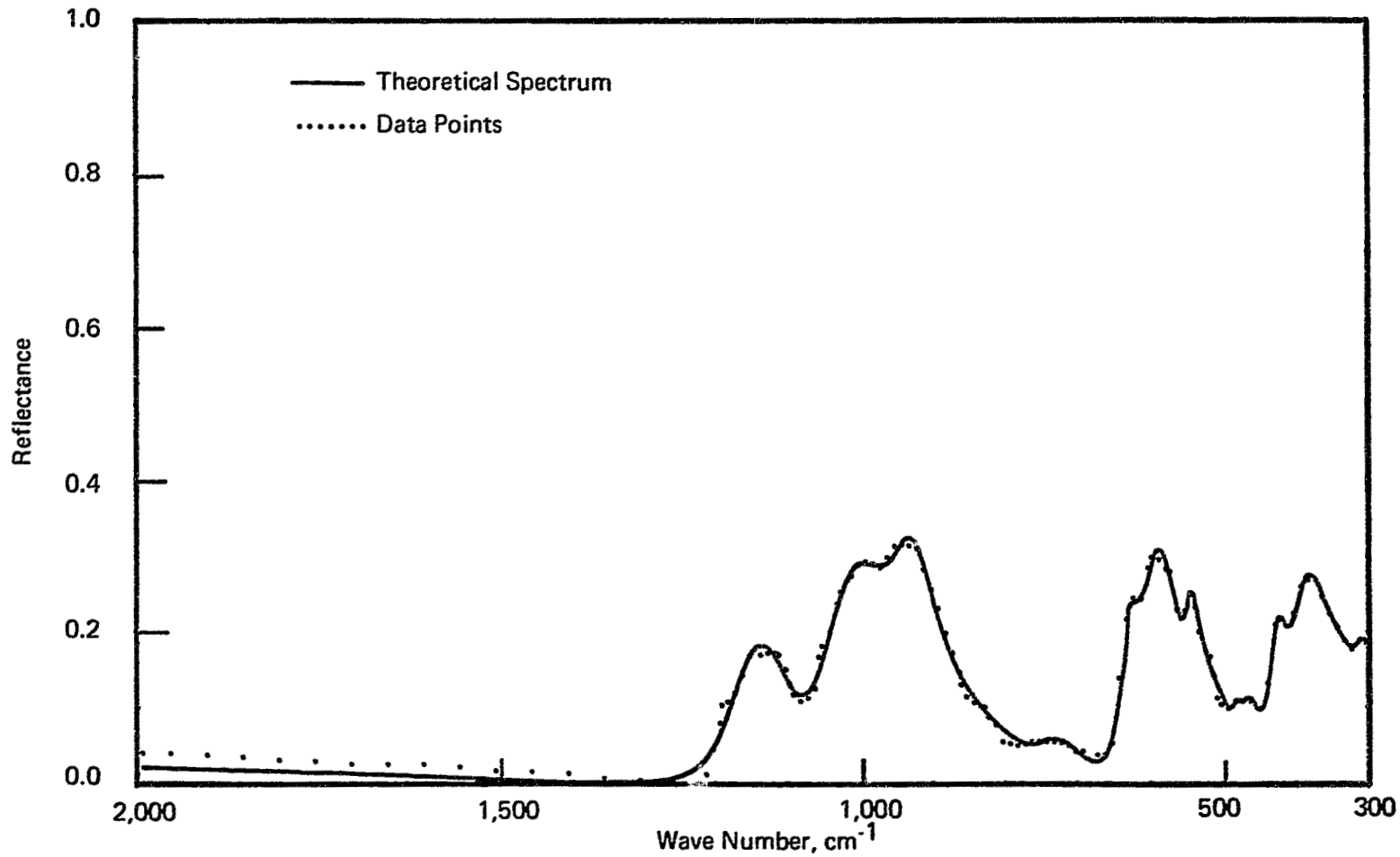
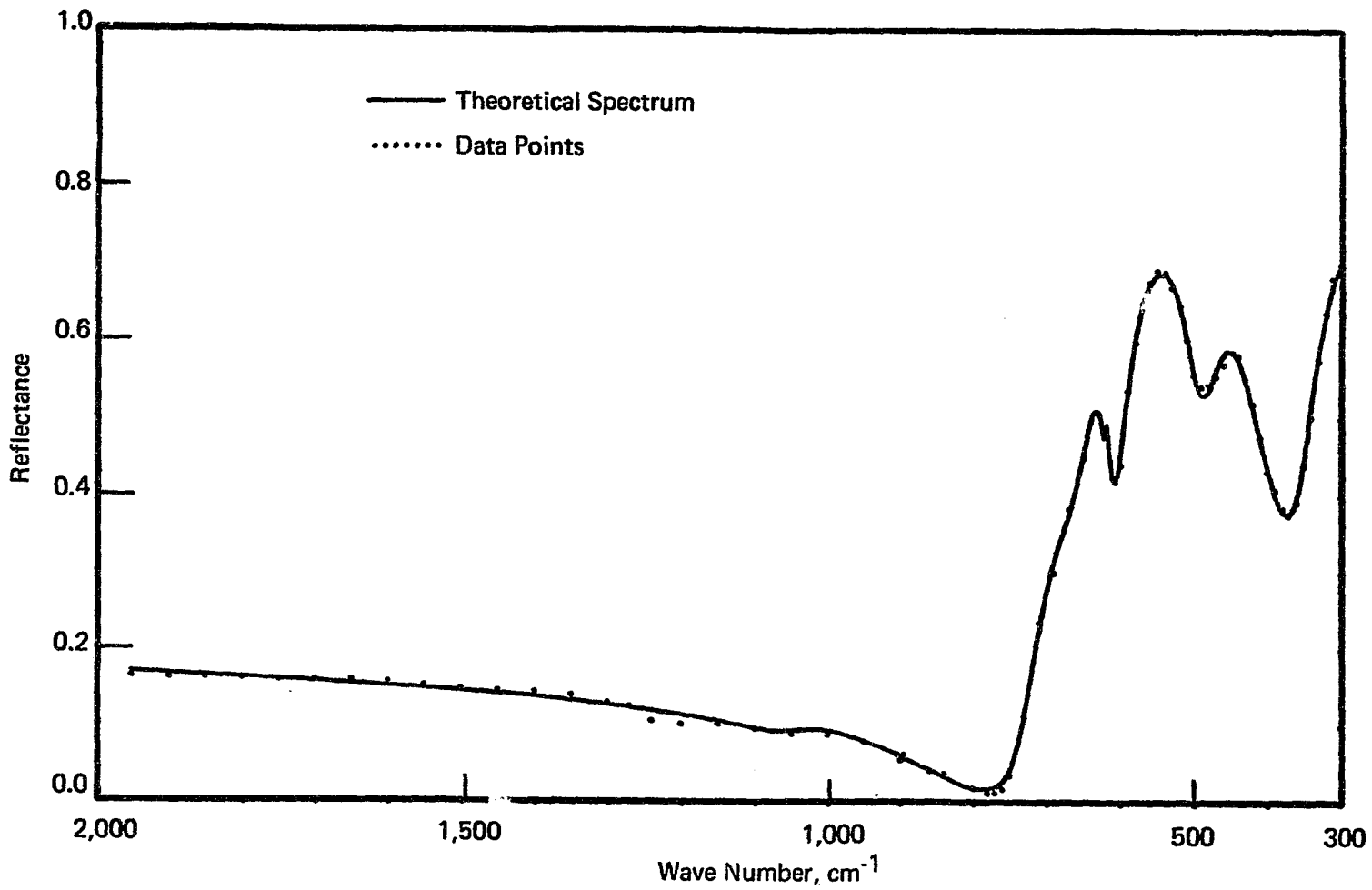FIGURE 3   REFLECTANCE SPECTRUM OF BYTOWNITE FITTED WITH TWELVE LORENTZ LINES

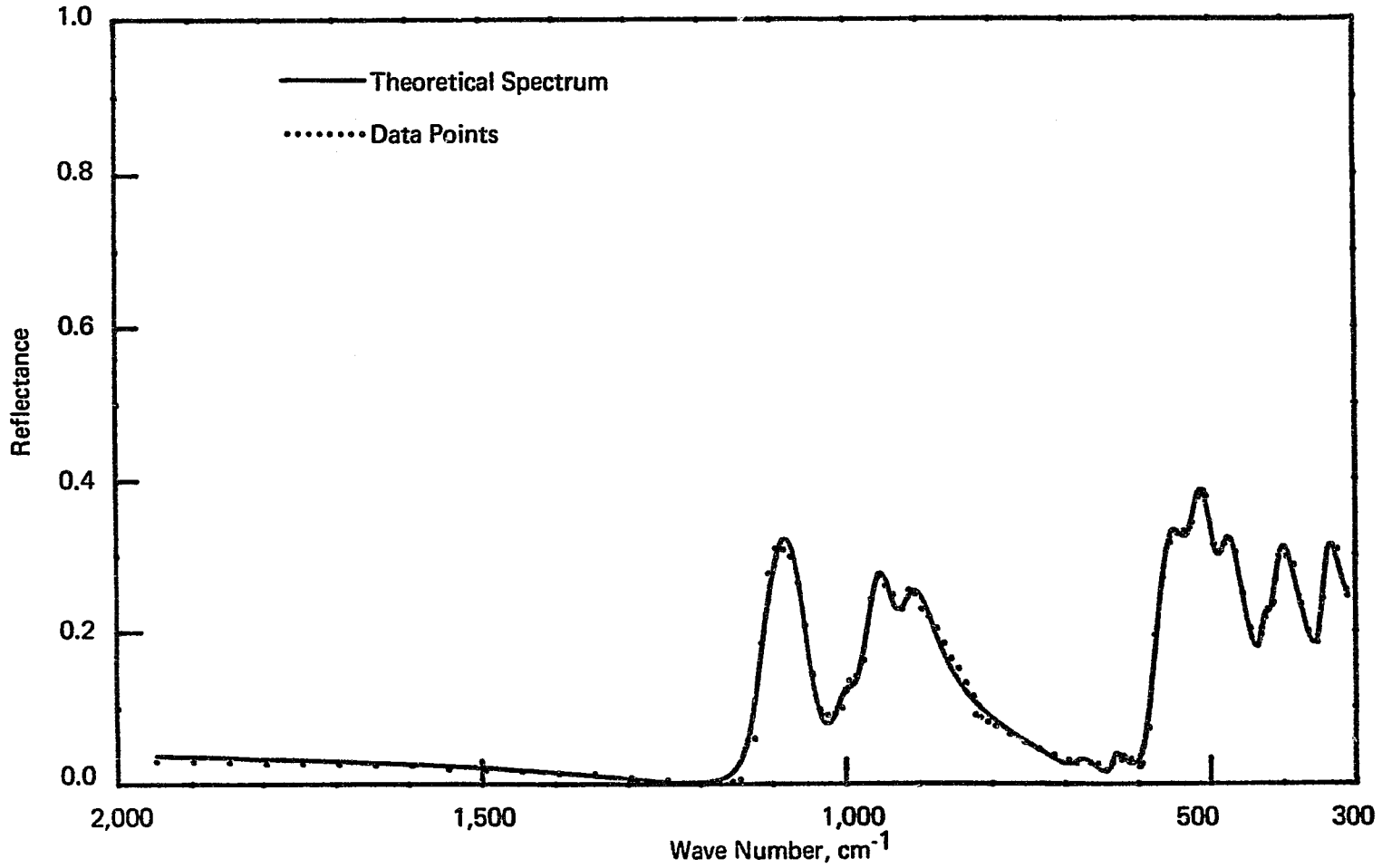FIGURE 4   REFLECTANCE SPECTRUM OF ILMENITE FITTED WITH SIX LORENTZ LINES

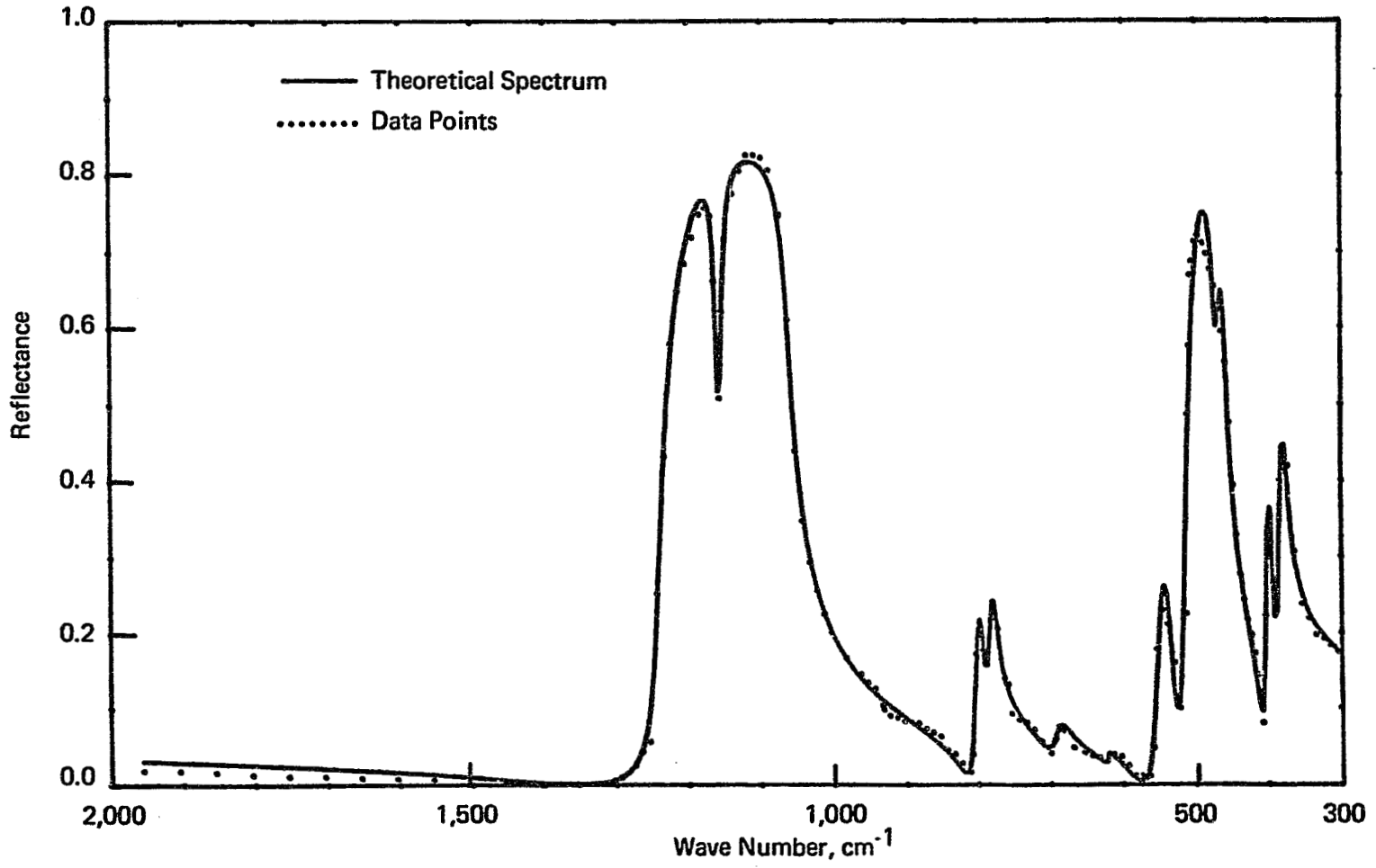FIGURE 5   REFLECTANCE SPECTRUM OF AUGITE FITTED WITH TWELVE LORENTZ LINES

FIGURE 6   REFLECTANCE SPECTRUM OF QUARTZITE FITTED WITH TEN LORENTZ LINES

As mentioned previously a very important practical consideration is the degree to which optical constants obtained from polished polycrystalline samples can be used to fit the spectra of powders. A relatively simple experiment to shed light on this problem was conducted by obtaining the optical constants of a fairly pure quartzite sample in our usual manner. The constants were then used together with our theory to predict the reflectance of powdered quartz. Figure 7 shows the calculated reflectance spectra of quartz for 20 μm and 60 μm particles using the optical constants derived from our quartzite sample and those derived by Spitzer and Kleinman[10] for pure quartz. This comparison circumvents any problems associated with theory itself and so should indicate what we wish to know about the optical constants alone.

The first and most obvious conclusions are that the calculated spectra resemble each other moderately well but that the reflectance level calculated using the pseudo optical constants (quartzite) is quite consistently below that calculated from the "true" values. This is likely to be due to the scattering from discontinuities in the surface of the polished quartzite sample which would reduce the measured reflectance in spectral regions where quartz is opaque owing to the surface microcracks, pores, and grain boundaries which would scatter some radiation out of the "specular" angle measured by the spectrometer. In regions where quartz is relatively transparent this effect is likely to be overwhelmed by additional energy scattered by underlying surfaces of the crystallites into the measured beam.

For the purposes of this discussion we should identify the reststrahlen bands of quartz as those regions where quartz is quite opaque. These are the bands between 350 cm^{-1} and 550 cm^{-1}, the doublet near 800 cm^{-1}, and the bands between about 1075 cm^{-1} and 1250 cm^{-1}. The bands near 650 cm^{-1}, 730 cm^{-1}, and 900 cm^{-1} represent regions of high transparency for quartz and, as with the data in the highest frequency regions shown in the spectra, give higher reflectances for small particle sizes owing to additional scattering by the greater number of interfaces encountered before the radiation can be absorbed.
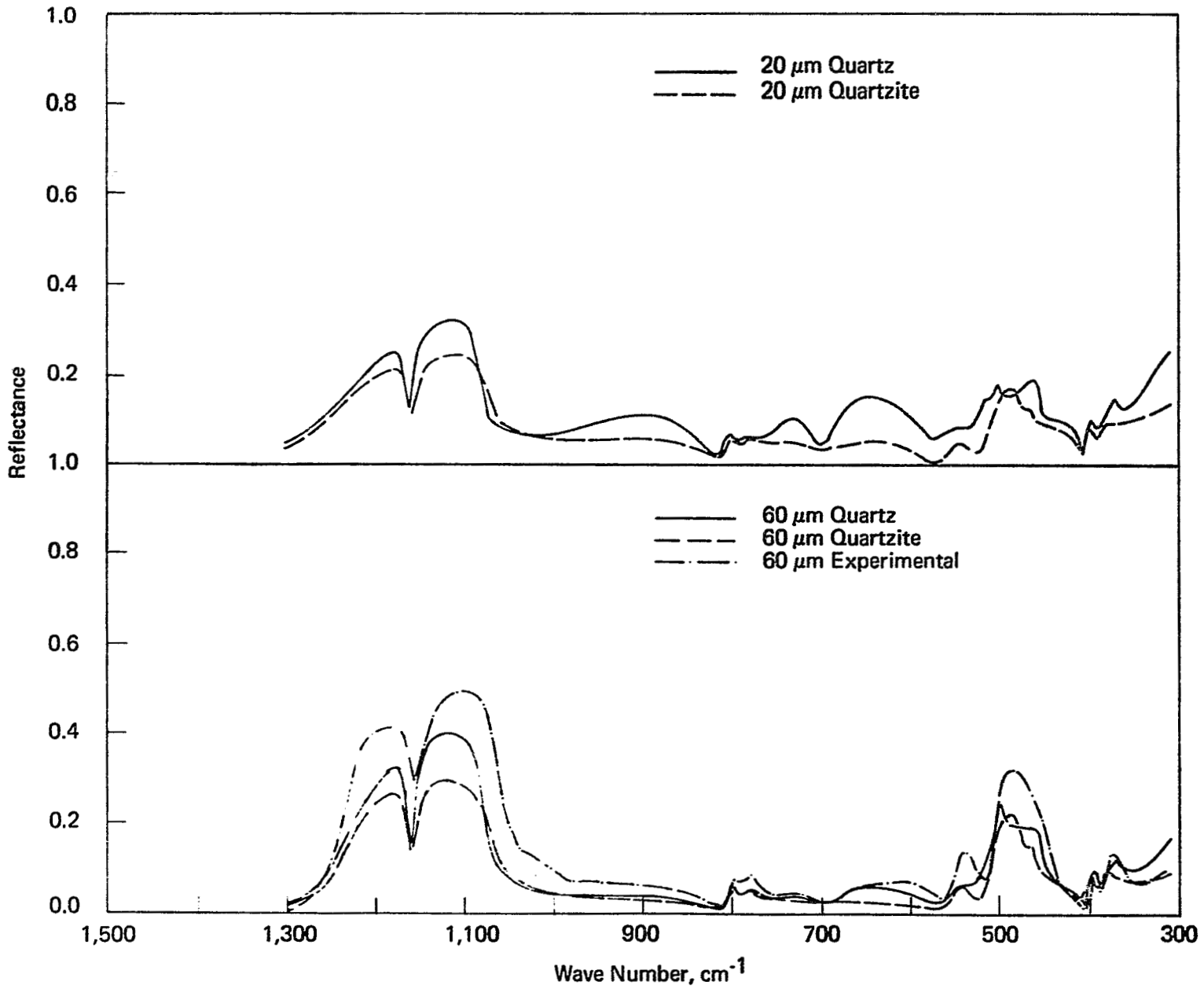
17

Arthur D Little, Inc.

**FIGURE 7   COMPARISON OF CALCULATED SPECTRA OF QUARTZ
POWDER USING THE OPTICAL CONSTANTS OF QUARTZ AND QUARTZITE**

The latter bands in particular are much more noticeable in the spectrum calculated from the true optical constants, and the reason is made apparent by the following comparison of values of the absorption index, k for the two orientations of quartz with the quartzite value.

$\nu(cm^{-1})$	$k(E \perp C)$	$k(E \parallel C)$	k(Quartzite)
650	.0109	.0127	.0542
730	.0205	.0231	.0723
900	.0169	.0153	.0393

The large values of k obtained for quartzite arise from an apparent increase in the specular reflectance in these regions caused by scattering from underlying discontinuities. In deriving the optical constants this enhanced reflectance has been interpreted as an increase in the Fresnel reflectance of the polished surface. This in turn has led to a spuriously high value of k.

Experimental data for 60 μm powder from our previous work[4] is included in Figure 7, and the calculated spectrum from the true optical constants can be seen to represent these features more accurately while the results are somewhat more mixed for the reststrahlen bands. A comparison of the data for our whole series of experimental quartz powders[4] (20 μm samples were not run) shows that these non-reststrahlen bands do become much more important as particle size is diminished and must be well represented for such sizes.

Arthur D Little, Inc.

IV. SPECTRA OF ANALOG POWDERS

The spectra of our powdered samples have been run in emission using our Michelson Interferometer Spectrometer System as previously described.[4] The data are shown as reflectance (R = 1-ϵ) to facilitate theoretical comparisons.

Figure 8 shows a comparison of the measured spectrum of the mare glass and the calculated theoretical spectrum. In order to simulate the measured particle size distribution given us by Dr. McKay for the glass powder sample we used the following values:

Measured Distribution		Calculation Values	
0.5-1mm	6.0%		
0.25-0.5mm	8.2	300μm	22.9%
150-250μm	8.7		
90-150μm	11.7	100μm	16.1
75-90μm	4.4		
45-75μm	13.1	50μm	24.0
30-45μm	10.9		
20-30μm	10.0		
15.6-20μm	5.7	15μm	31.0
7.8-15.6μm	15.3		
3.9-7.8μm	5.3	5μm	6.0
2.0-3.9μm	0.7		

We have previously found that such simplification in the distribution is sufficiently accurate especially at the larger particle sizes. The measured particle size distribution resulted from sieving and recombination by Dr. McKay and his associates for particle sizes greater than 30 μm. Below that value an estimate was made based on his experience with grinding operations. The packing fraction was taken to be 0.54 from measurements of the bulk glass density and the density of the powder. The experimental measurements were made under a nitrogen atmosphere at ambient pressure. This resulted in a temperature gradient through the powder of about 6°/cm. These conditions result in a rather good fit of the calculated and measured spectra between 350 and 1200 cm^{-1}. Beyond these limits the fit deteriorates owing probably to the limits of the spectrum measured on the bulk sample for the optical
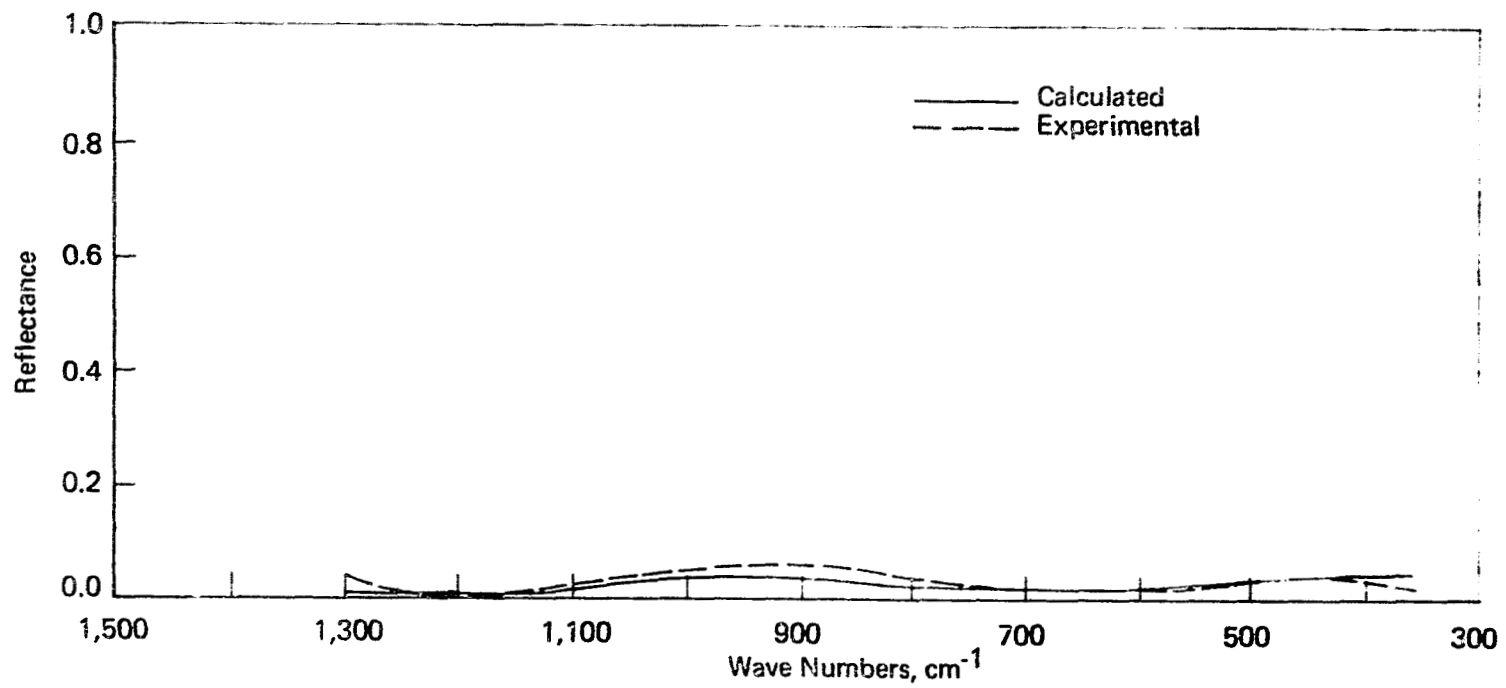
20

FIGURE 8   REFLECTANCE SPECTRUM OF ANALOG MARE GLASS

constants. The data show very modest spectral contrast as was expected from results on other glass samples.

We obtained the optical constants of dunite during this work as those measured by Vincent[15] were believed to be for a preferentially oriented sample. Data on the optical constants of pure single crystal forsterite are also available,[16] but we were uncertain as to the magnitude of band shifts that might occur owing to the replacement of Mg^{++} ions by Fe^{++} in dunite. A comparison of theoretical spectra for 60 μm powder using Vincent's optical constants, those of Servoin[16] for forsterite (assuming a randomized mixture of the three possible orientations of the crystallites),and our new values is shown in Figure 9. The spectrum from our optical constants is quite similar to that produced by Vincent's optical constants but gives more structure especially in the low frequency region. This structure is shown to be real by the comparison of our data with that for pure forsterite. The noticeable discrepancy when our data is compared with the pure forsterite data at the high frequency end is believed to be explained by the same defect in the optical constants discussed in the previous section for quartzite. Examination of this data together with transmission data given by Lyon[12] suggests possible correlations between the Fe^{++} contents and the bands near 980 and 610 cm^{-1}. The correlation mentioned by Estep[7] near 418 cm^{-1} is not clearly shown but may be present in our data.

In Figure 10a we show the measured spectra of 150-250 μm dunite, 0-30 μm dunite, and a simulated lunar mixture of particle sizes of dunite according to the same distribution given for the glass. As this report was in the final stages, we received the 0-30 μm particle size counts for the pyroxenite, dunite, and bytownite samples. These counts indicate that a somewhat better simulation would have weighted the small particles more heavily (i.e., 15 μm, 26%; and 5 μm, 11%), but such a change is not expected to have much effect. The packing fractions given in the figure result from measurements of the densities of the powders and the known density of the mineral.
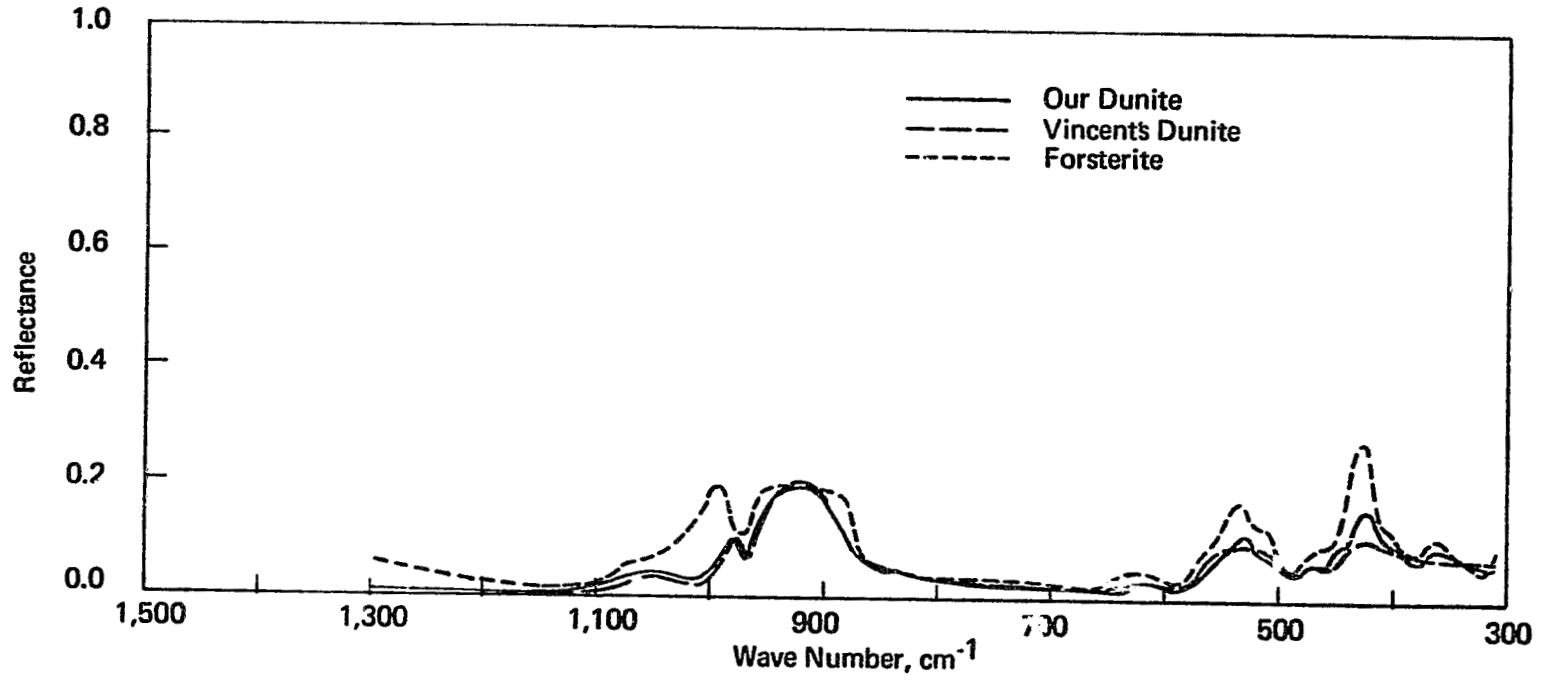
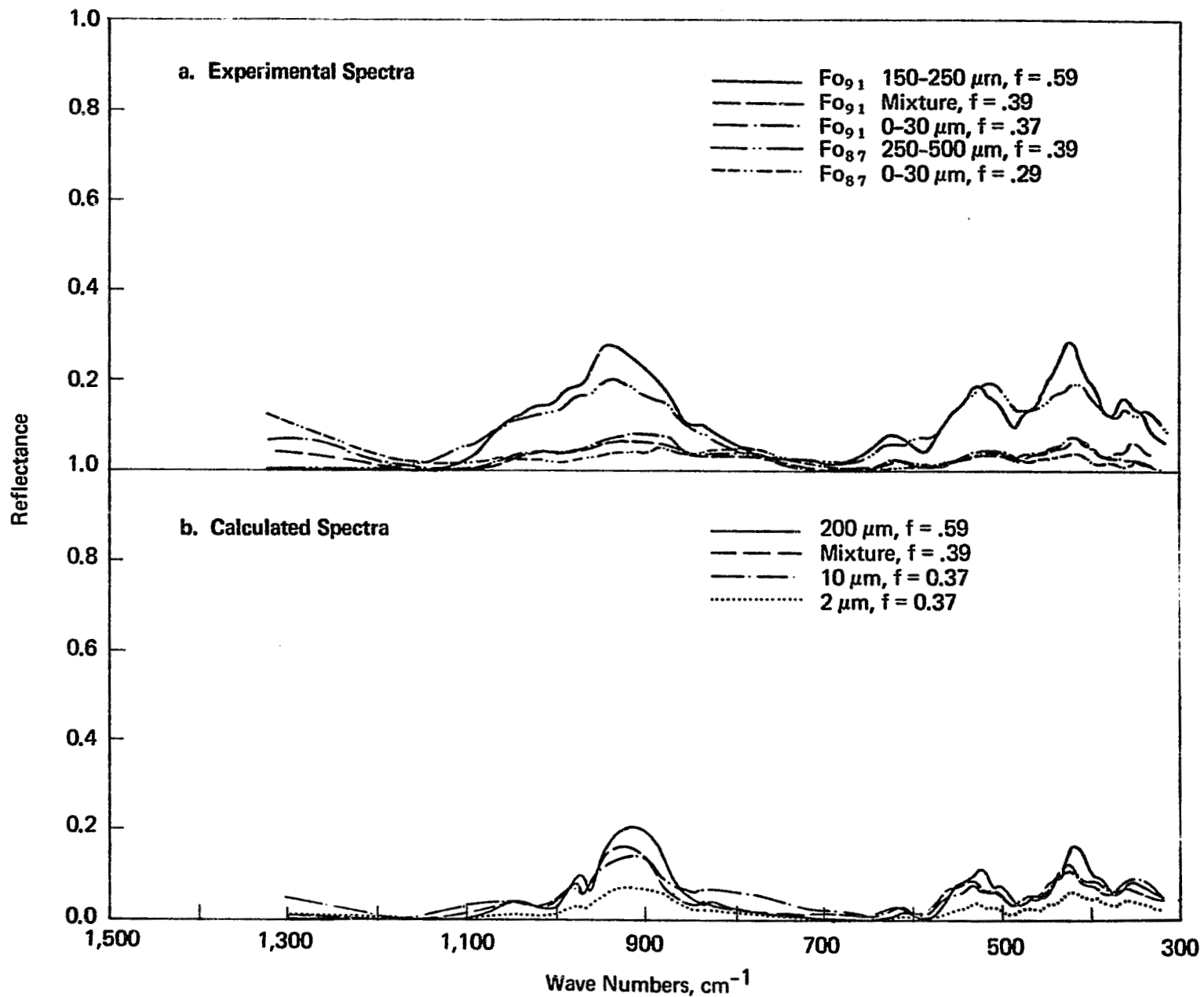FIGURE 9   COMPARISON OF CALCULATED SPECTRA OF OLIVINES

Arthur D Little, Inc.

FIGURE 10   REFLECTANCE SPECTRA OF DUNITE

Figure 10b shows the calculated spectra of 200 μm, 10 μm, and 2 μm dunite. The latter two runs were made in order to represent the less than 30 μm sample as we were uncertain of the measured distribution below 30 μm at the time. Together they well represent the observed spectrum and we believe the proper distribution would also. The 200 μm sample is a good fit to the experimental data except that the general spectral level for the calculated spectrum is a bit too low, probably the result of scattering loss in the measurements which led to the optical constants as described in the last section. The spectrum of the particle size mix is quite dominated by the 0-30 μm sample as shown in Figure 10a.

Several runs of the Fo_{87} dunite were also made and are shown in Figure 10a. They have similar band patterns with some differences from our Fo_{91} dunite. We do not feel these differences are significant with respect to the Fe++ content.

Figure 11a shows the experimental spectra obtained for 250-500 μm, 0-30 μm, and a simulated lunar particle size mixture of bytownite. Theoretical runs are shown in Figure 11b. The 250-500 μm bytownite data were simulated by a 350 μm theoretical run with excellent results. As before, the experimental spectrum has a higher reflectance level than the theoretical simulation probably owing to the scattering loss sustained in the measurements of the optical constants. When the 0-30 μm spectrum was run, a band near 820 cm^{-1} appeared that the theoretical run (5 μm) does not produce. We first associated the presence of this unexplained band with the presence of some impurity in the sample, but a magnetic separation of dark particles and rerun of the purified sample showed the offending band to have been essentially unaffected. For the 0-30 μm sample, the rise in reflectance observed experimentally at frequencies just higher than the Christiansen frequency is also not well fit. The simulated lunar mix strongly resembles the 0-30 μm sample indicating as we have noted before[4] that it is common for a relatively small amount of fine particles to exert a disproportionate effect on the spectrum of a polydisperse sample. The poor fit at high frequencies and near 820 cm^{-1} appear simultaneously, and we postulate that they are
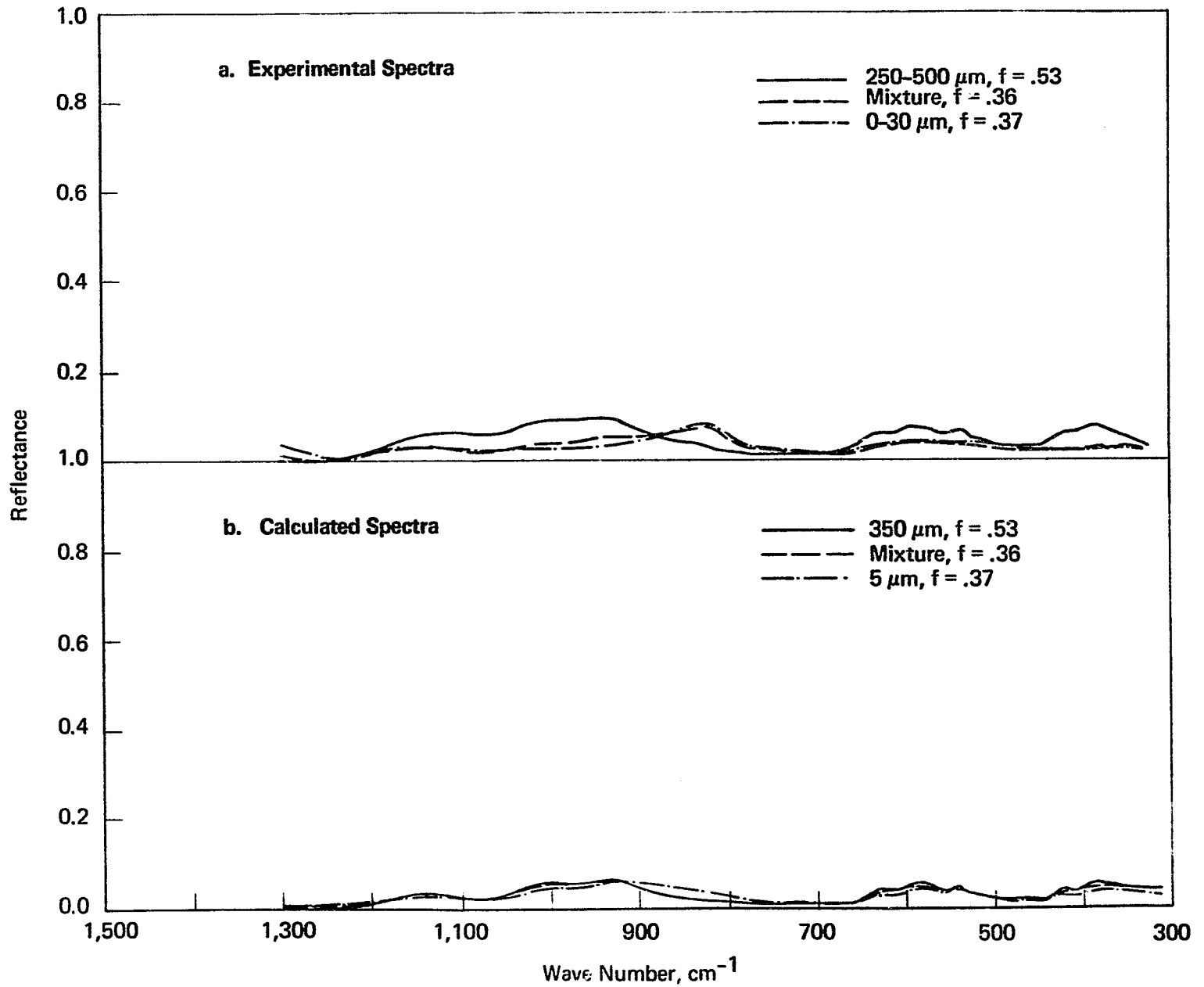
25

FIGURE 11   REFLECTANCE SPECTRA OF BYTOWNITE

26

Arthur D Little Inc

due to the same cause. As previously discussed, if the calculated value of the absorption index is not sufficiently small, bands created by scattering of relatively transparent particles will not be produced in the theoretical spectrum. As can be seen in Lyon's[12] transmittance spectra, the region of the offending band is indeed relatively transparent in all feldspars. Our calculated value of the absorption index shows a local minimum of 0.241 at 805 cm^{-1}. This would not be low enough to produce the band required, but another factor of five would undoubtedly have a good chance of so doing. Such errors in the absorption index were shown in the experiment with quartzite. If this explanation is valid, we would expect the band to disappear in the spectrum of a mixture of minerals as absorption by other minerals would destroy this type of band.

Figure 12a shows the spectra of 90 μm - 1 mm, 0-30 μm, and a simulated lunar particle size mix of the diopsidic pyroxenite sample. We ran the wide distribution of coarse particles as we did not have enough sample to run smaller particle size cuts. Both the 0-30 μm and the mixture data show small tilts in the overall spectrum. These are due to an experimental error that occurs occasionally, but we have not yet located its origin. Figure 12b shows our theoretical simulations of these spectra. As with our other minerals, the fit of the coarse spectrum to the data is quite good except for the absolute spectral level. However, the 0-30 μm spectrum shows the poorest fit we have ever seen with our present theory. The spectrum of the mixture, however, is fitted much better particularly by an 8 μm calculation rather than that for the simulated mixture. The mixture size parameters involved a limited set of measurements of the 0-30 μm fraction rather than the numbers given us by Dr. McKay. For this case only we used:

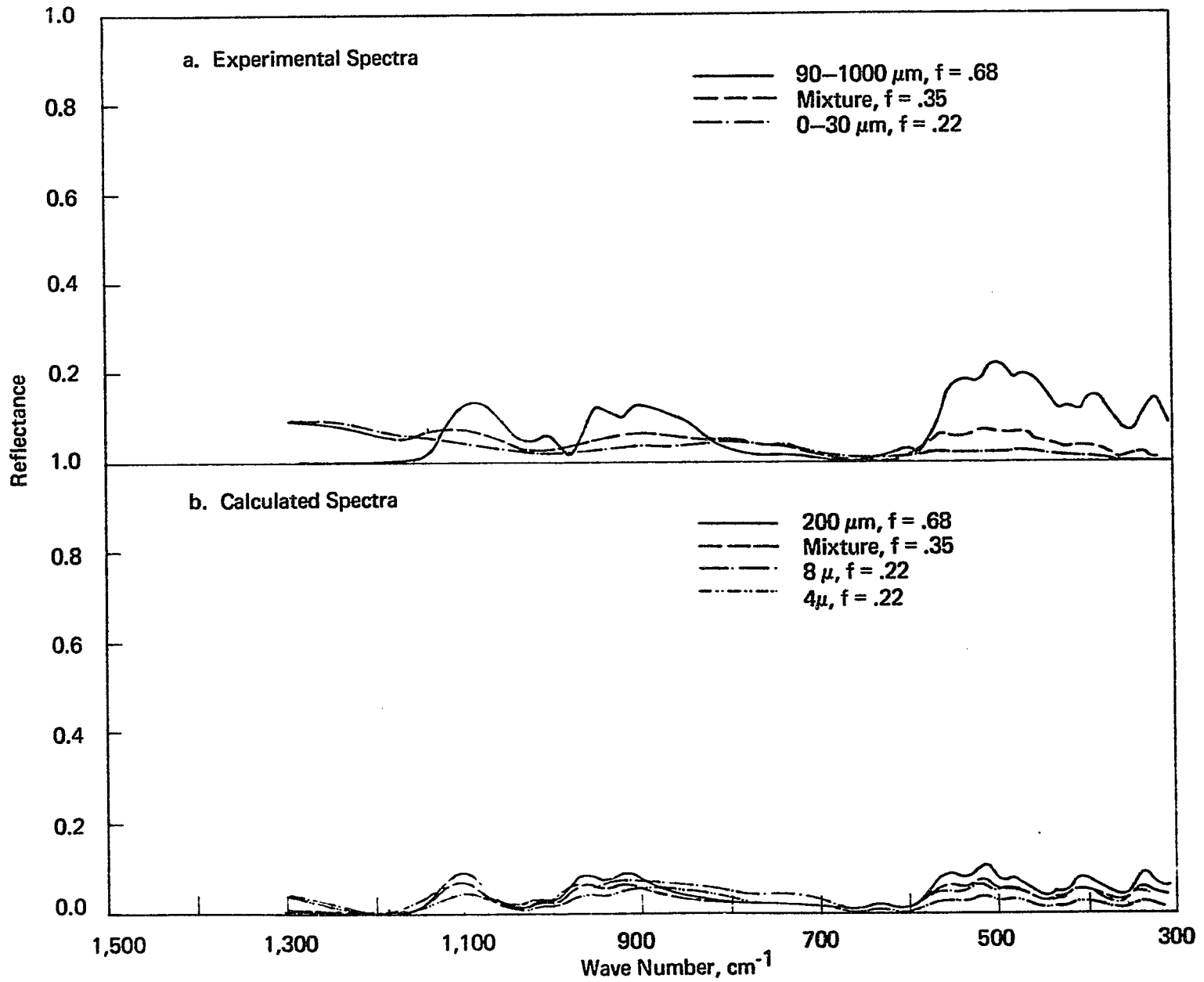| Calculation Values	
500 μm	34%
60 μm	29%
20 μm	28%
5 μm	9%

27

FIGURE 12   REFLECTANCE SPECTRA OF PYROXENITE

Arthur D Little, Inc.

The improved fit by the 8 μm calculation together with the quartzite and bytownite results suggests the likely explanation. The principal difficulty with the 8 μm fit to the mixture data occurs at the high frequency end of the spectrum where our calculated value of k is not as small as it should be. Such difficulties are amplified when the calculation is made for a mixture of sizes and are compounded by difficulties in the 800 and 450 cm^{-1} regions. As before, these are regions of relative transparency in diopside[12] and show local minima in our values of k. As the bands that we are lacking in the calculations are maximized for relatively fine powders (they disappear again in powders so small as to be well into the region of the fine particle theory), the 8 μm calculation affords a better chance to show them than the calculation for the true mix. Once again the importance of correct values of k for the "transparent" regions is emphasized. With this hypothesis in mind we can go on to an attempt to rationalize the trouble with our 0-30 μm fit. The difficulties can now be observed (compare the 4 μm theoretical run) to be still further exacerbated in the regions mentioned above and now to include the region around 1030 cm^{-1} as well. This region is shown by Lyon's data[12] and our values of k to have a similar character to the regions discussed though quantitatively less significant. The extremely poor fit shown here was evidently caused by the same difficulty as above (k not calculated sufficiently low in certain spectral regions) but exacerbated by the lack of relatively large particles (as in the mix) where individual particle absorption by the large particles present in the mix ameliorated the difficulty.

It should be noted that the seriousness of this problem of precise values for the optical constants will be somewhat lessened in mixtures as the problem principally occurs when a spectral region is encountered where significant particle scattering without attendant absorption is found. This is much less likely to occur for mixtures of minerals than for any pure substance. Nonetheless it is very important that improved optical constants be obtained in future work.

Arthur D Little Inc.

In Figure 13 we have plotted our experimental and theoretical results for a lunar analog mixture made up to approximate the lunar soil 12063. The fit between theory and experiment shows difficulties at the high frequency end, in the region around 800 cm^{-1} and to a smaller degree near 450 cm^{-1}. These occur due to the previously mentioned problem with the pyroxenite which dominates the mixture. It should be noted that the 800 cm^{-1} feature of fine bytownite cannot be observed in the mixture spectrum as predicted. The level observed is excellent, and we feel confident that the origin of the problem is well understood and would be remedied by improved optical constants. The high frequency region is very poorly fit as all the components are relatively transparent there, and so do not ameliorate the problem for each other. We include in the figure the experimental spectrum of the same sample taken under a partial vacuum of about 0.14 Torr. While this is not a low enough pressure to simulate the lunar vacuum and hence lunar thermal gradients (the polarity is incorrect for lunar daytime experiments), the comparison does serve to show that a greatly increased temperature gradient in the sample (32 °/cm vs. 6.3 °/cm as estimated by our differential thermocouple technique[4]) does not seriously alter the spectral signature of the sample. We had also reached this conclusion in our previous work.[17] It should be noted that for the high gradient sample our usual methods of defining the surface temperature by either the thermometry[4] or the Christiansen frequency technique[4] are invalid so that this spectrum has been arbitrarily set at a level where its emittance is the same as the nearly isothermal sample in the principal reststrahlen region. This involves an 8° error in the thermometry but basically represents only a level effect and does not significantly affect the signature.

Figure 14 shows the same kind of fit between theory and experiment for a simulated mature soil made up of the sample of Figure 13 and an equal amount of the Mare glass sample. The fit here is somewhat better than in Figure 13 owing to the reduced effects of the trouble inherent in the pyroxenite calculations. The general conclusion that mature and immature soils can be distinguished even if they have similar
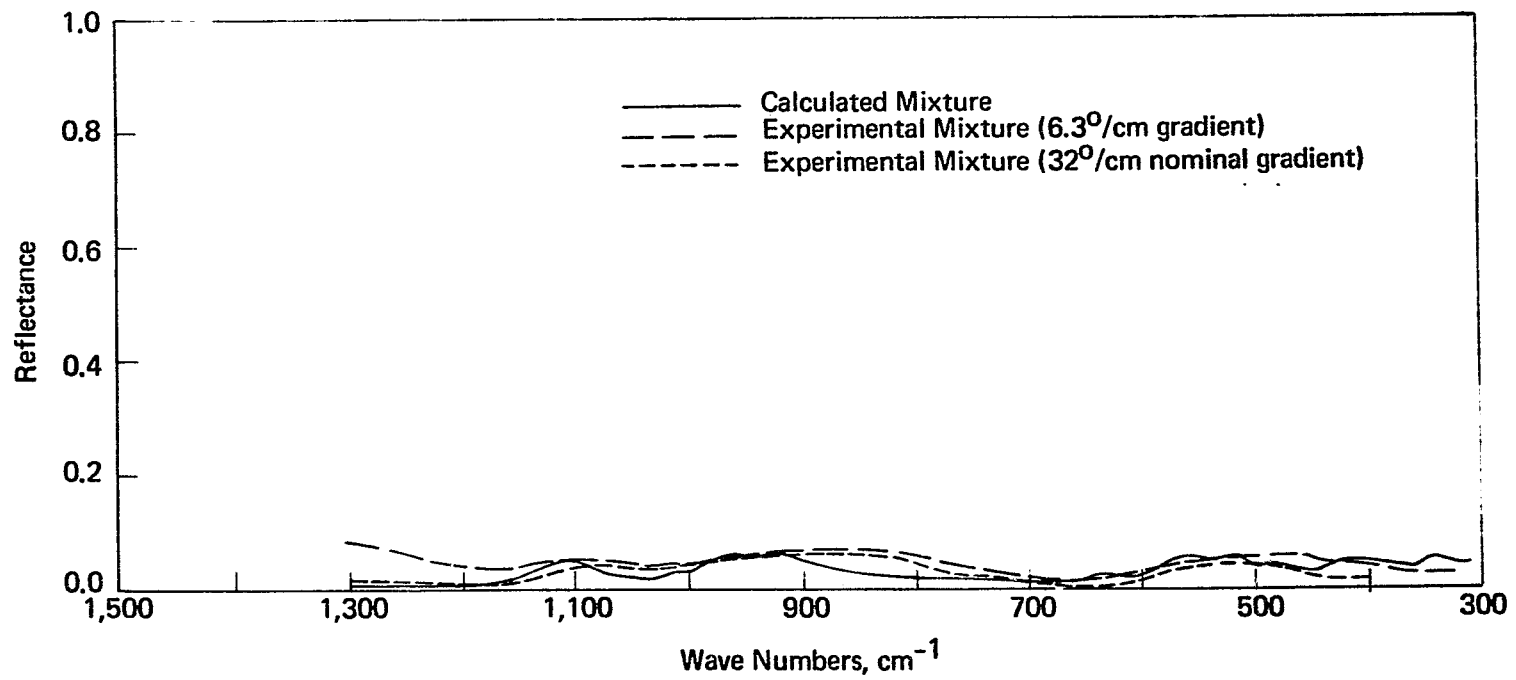
FIGURE 13   REFLECTANCE SPECTRA OF IMMATURE LUNAR SOIL ANALOG

Arthur D Little Inc

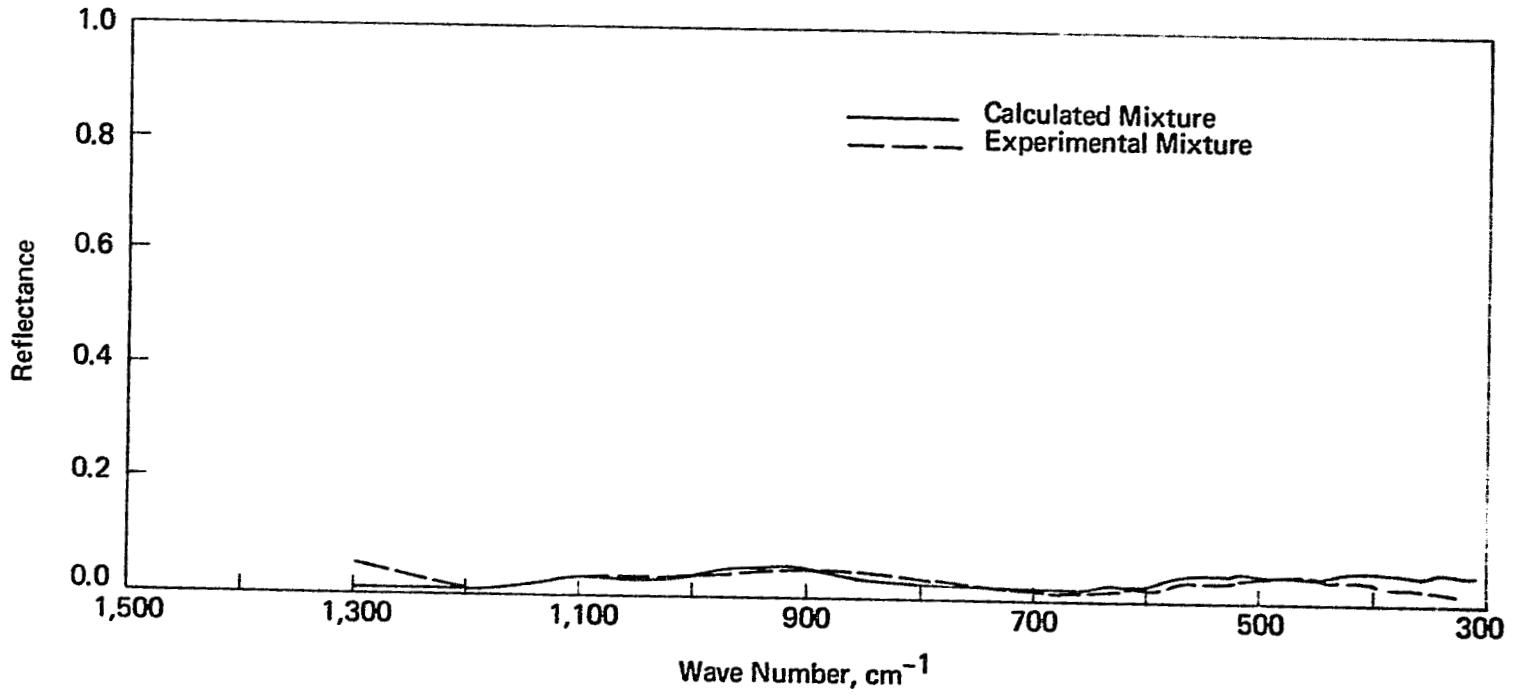FIGURE 14   REFLECTANCE SPECTRA OF MATURE LUNAR SOIL ANALOG

chemistries is shown in a comparison of the results of these two experiments in Figure 15 where the level change in the reststrahlen bands can be seen in both theory and experiment. This was predictable _a priori_ from the knowledge that glass spectra generally show less contrast than crystal spectra.
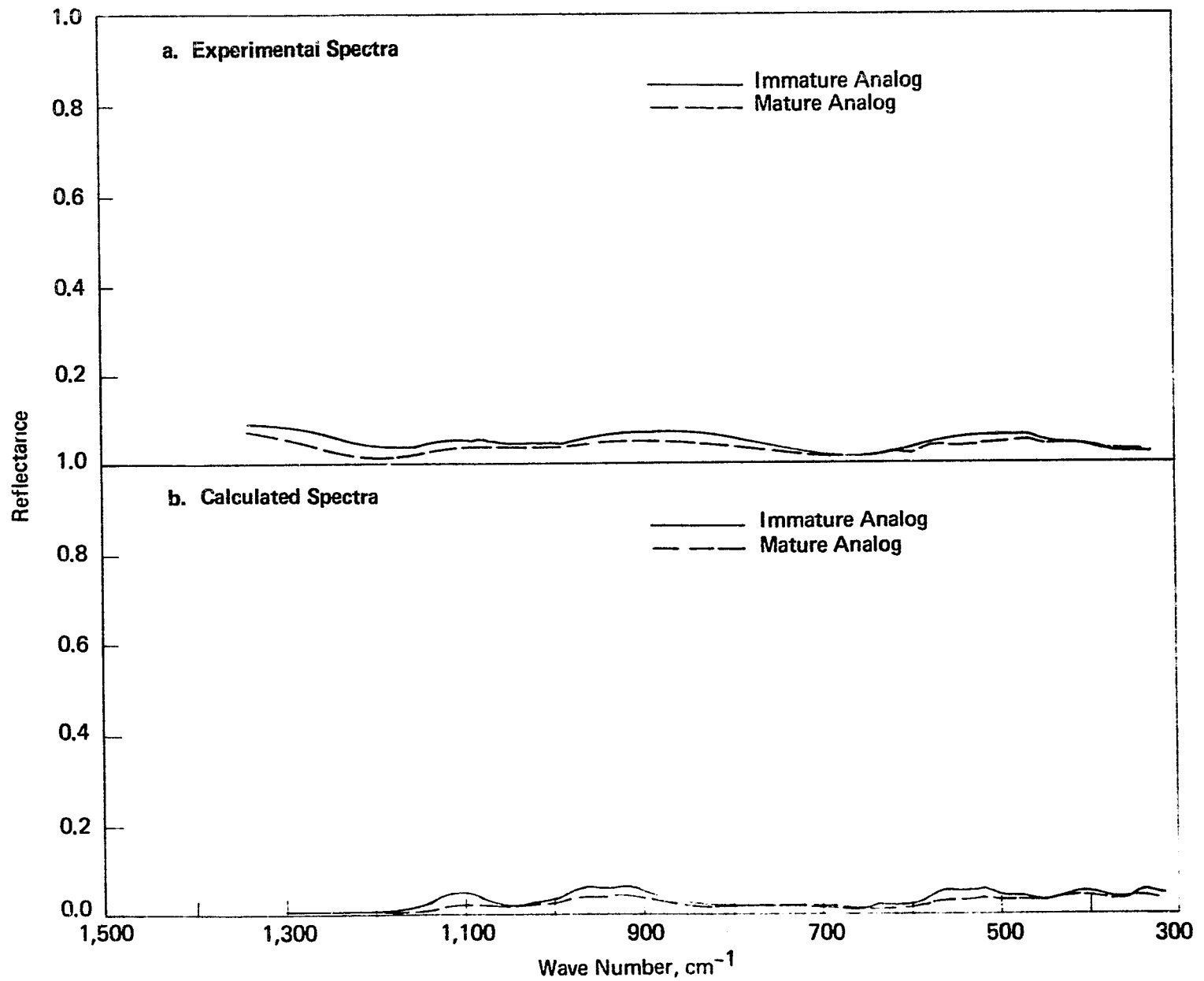
Arthur D Little Inc.

FIGURE 15   COMPARISON OF SPECTRA OF MATURE AND IMMATURE SOIL ANALOGS

34

Arthur D Little Inc

V. SMALL METALLIC INCLUSIONS

In our early discussions with Dr. McKay we became acquainted with a problem which will be most important for real lunar samples and concerns the significant observed amounts of small iron particles found throughout many samples. Dr. McKay expressed considerable pessimism concerning the possibility of preparing an analog of lunar agglutinates because of these iron particles (50-100A diameter). However, our theoretical treatment for small particles shows that we can easily simulate the effect of such particles, as their extremely small size precludes their contributing significant scattering in the infrared region. Their absorption can easily be incorporated into our theoretical program knowing only their concentration and optical constants. It is worth noting that the cross section for absorption owing to these particles is likely to be significantly less in the infrared region than in the visible region, where they are thought to contribute to the low albedo observed.

We have found[18,19] a dispersion equation for use in our program for small iron particles, viz:

$$m^2 = \varepsilon_\infty + \frac{iC_1}{\nu} + \sum_{j=1,2} \frac{S_j}{i\left(\frac{\nu}{\nu_j}\right) - \left(\frac{\nu}{\nu_j}\right)^2}$$

where
$\varepsilon_\infty = 1.15$
$C_1 = -1.440 \times 10^5$ cm
$S_1 = 5.616$
$S_2 = 4.284 \times 10^4$
$\nu_1 = 2.564 \times 10^4$ cm^{-1}
$\nu_2 = 1.333 \times 10^2$ cm^{-1}

We have coded an option to use this equation in our program when real lunar samples are obtained.

VI. CONCLUSIONS AND SUGGESTIONS FOR FURTHER WORK

The results of our studies of the emittance of analogs of lunar minerals indicate that, as expected, our theory of particulate scattering is a valuable tool for interpreting the remote infrared spectra of planetary surfaces. The most important single result of this work has been the evidence that the goodness of fit between theory and experiment is critically dependent on the accuracy of the catalogue of optical constants of the relevant minerals. In particular the values of the absorption index, k, in regions of relatively high transparency must be properly calculated to avoid errors in band shapes for soils that contain significant amounts of small particles (<50μm). The technique used in this work fails to properly represent k in transparent regions when the samples are polished polycrystalline minerals. Improved measurements of the optical constants are very important, and assuming the solution of the optical constant problem, the method of remote sensing of planetary surface composition discussed in this report appears well feasible. We suggest that:

1. Similar experiments be made on real lunar soils and theoretical simulations be compared with the experimental data.

2. The effects of small metallic particles modeled during this work should be tested on real lunar soils.

3. Further theoretical and experimental work on the quantitative effects of thermal gradients should be carried out.

4. Improved methods be explored for improving the optical constants of the catalogued minerals.

5. The optical constants of more lunar analog minerals be obtained.

VII. REFERENCES

1. W. W. Coblentz, Investigations of Infrared Spectra, Carnegie Institution of Washington (1905)

2. G. R. Hunt and R. K. Vincent, J. Geophys. Res. 73, 6039 (1968)

3. A. G. Emslie and J. R. Aronson, Appl. Opt. 12, 2563 (1973)

4. J. R. Aronson and A. G. Emslie, Appl. Opt. 12, 2573 (1973)

5. J. R. Aronson and A. G. Emslie, "Applications of Infrared Spectroscopy and Radiative Transfer to Earth Sciences," in Infrared and Raman Spectroscopy of Lunar and Terrestrial Minerals, Acad. Press (1975) Ed. C. Karr, Jr.

6. P. A. Estep, J. J. Kovach and C. Karr, Jr., Proc. Second Lunar Sci. Conf. 3, 2137, M.I.T. Press (1971)

7. P. A. Estep, J. J. Kovach, P. Waldstein and C. Karr, Jr., Proc. Third Lunar Sci. Conf. 3, 3047, M.I.T. Press (1972)

8. C. Pieters, J. W. Head, T. B. McCord, J. B. Adams and S. Zisk, Proc. Sixth Lunar Sci. Conf. 2689 (1975)

9. J. R. Aronson and P. F. Strong, Appl. Opt. 14, 2914 (1975)

10. W. G. Spitzer and D. A. Kleinman, Phys. Rev. 121, 1324 (1961)

11. G. Bird and M. Parrish, Jr., J. Opt. Soc. Am. 50, 886 (1960)

12. R. J. P. Lyon, NASA TN D-1871 (1963)

13. E. E. Angino, Kansas Geol. Surv. Bull., 194, Pt. 1 (1969)

14. J. R. Aronson and A. G. Emslie, The Moon 5, 3 (1972)

15. R. K. Vincent, NASA, CR-ERIM 190100-30-T (1974)

16. J. L. Servoin and B. Piriou, Phys. Stat. Sol. 55, 677 (1973)

17. J. R. Aronson, A. G. Emslie, L. H. Roach, E. M. Smith and P. C. von Thuna, "Development of a Theory of the Spectral Reflectance of Minerals," A.D.L. Report on Contract NAS9-10875, January 1, 1972

18. S. Roberts, Phys. Rev. 100, 1667 (1955)

19. R. A. Seban, J. Heat Trans. 173 (May 1965)